Electronic Supplementary Material (ESI) for Journal of Materials Chemistry A.

Supporting Information

For

Stabilizing Nickel-Rich Layered Cathode Materials by a High-Charge Cation Doping Strategy: Zirconium-Doped $LiNi_{0.6}Co_{0.2}Mn_{0.2}O_2$

Florian Schipper[a,#], Mudit Dixit[a,#], Daniela Kovacheva[b], Michael Talianker[c], Ortal Haik[a], Judith Grinblat[a], Evan M. Erikson[a], Chandan Ghanty[a], Dan T. Major[a,z], Boris Markovsky[a,z], Doron Aurbach[a]

[a]*Department of Chemistry and the Lise Meitner-Minerva Center of Computational Quantum Chemistry, Bar-Ilan University, Ramat-Gan 52900, Israel*

[b]*Institute of General Chemistry, Bulgarian Academy of Sciences, Sofia 1113, Bulgaria*

[c]*Department of Materials Engineering, Ben-Gurion University of the Negev, Beer-Sheva 84105, Israel*

[z]Corresponding authors.

[#]These authors contributed equally to this work.

E-mail: markovskyboris22@gmail.com Tel. + 972 3 531 88 32; Fax. + 972 3 738 40 53

E-mail: majort@biu.ac.il Tel. + 972 3 531 73 92; Fax. + 972 3 738 40 53

Contents

1. Experimental Methods

1.1. Synthesis of $LiNi_{0.6}Co_{0.2}Mn_{0.2}O_2$ and $LiNi_{0.56}Zr_{0.04}Co_{0.2}Mn_{0.2}O_2$ materials. Cathode materials, undoped and Zr-doped NCM-622, were synthesized *via* the solution combustion technique. Analytical grade $LiOH{\cdot}H_2O$, $Ni(NO_3)_2{\cdot}6H_2O$, $Co(NO_3)_2{\cdot}6H_2O$, $Mn(NO_3)_2{\cdot}4H_2O$, $Zr(NO_3)_2{\cdot}nH_2O$ (ZrO_2=43.5%) were used as oxidizers and sucrose ($C_{12}H_{22}O_{11}$) was used as a fuel for this reaction. The molar ratio between the nitrates and sucrose was calculated according to the principles of combustion reaction on the basis of the total oxidizing and reducing power of the metal nitrates and the sucrose. A small excess of lithium (~2%) is added based on our previous experience.[1] The metal nitrates and sucrose were dissolved in an optimal amount of distilled water to obtain clear

solutions and subsequently mixed in a single laboratory dish, which was then placed in a heater to slow evaporation of the water. Upon heating the solution, the self-igniting and exothermic reaction starts at around 400 °C. The combustion process produced a voluminous amorphous mass, which was heat treated at 400 ^{o}C for 1 h to ensure the burning of residual organic components. Contrary to the synthesis of spinel-type cathode materials, the layered ones need higher synthesis temperature.[2] XRD patterns in Figure S2 show the effect of increasing the annealing temperature on the evolution of the layered structure towards separation of TM ions and Li ions onto their respective planes. Rietveld analysis revealed, however, that the materials obtained after heat treatment at 600, 700 and 800 ^{o}C showed a high level of cation mixing between the Li and 3d-metal layers. For example the presence of 3d metal ions in the Li layer was found to be as high as 0.25 for the NCM-622 material heated at 700 ^{o}C.

1.2. Electrochemical measurements. Electrochemical tests were carried out in two- and three-electrode cells in a 2325 coin-type and pouch-type configuration with a Celgard, Inc. polypropylene separator. The working electrodes were composites of a mixture of $LiNi_{0.6}Co_{0.2}Mn_{0.2}O_2$ materials (undoped or Zr-doped), carbon black (CB) and polyvinylidendifluoride (PVdF) binder (80:10:10 by weight) on aluminum foil (from Strem). We prepared also thin-film working electrodes comprising only active $LiNi_{0.6}Co_{0.2}Mn_{0.2}O_2$ materials embedded into Al-foil by wiping. These electrodes were free from CB and PVdF, their thickness was ~0.5μ, as measured by the focused ion-beam technique. Lithium disks or plates and lithium chips served as counter and reference electrodes. Electrochemical cells were assembled in glove boxes filled with highly pure argon (VAC, Inc.). We used electrolyte solutions (high purity, Li battery grade)

comprising ethyl-methyl carbonate (EMC) and ethylene carbonate (EC) (weight ratio of 7:3) and 1M $LiPF_6$ from BASF. The content of hydrofluoric acid and water in the solutions was not more than 30 ppm and 10 ppm, respectively. After assembling, the electrochemical cells were stored at room temperature for 12 – 24 h to ensure a complete impregnation of the electrodes and the separators with the electrolyte solution. The electrochemical measurements were performed using standard equipment as described previously[8]. All the potentials in this paper are given vs. Li/Li^+. For statistical reasons, the measurements were repeated and the accuracy of the calculations of the electrodes' capacity was around 95%.

1.3. X-ray diffraction (XRD), transmission electron microscopy (TEM) and electron diffraction (ED) analyses. X-ray powder diffraction (XRD) measurements were performed using an AXS D8 Advance diffractometer from Bruker, Inc. (Germany) in the 2θ range from 10° to 110°, with a step size of 0.02°, at a 15 sec/step rate. The analysis of the XRD patterns was carried out using the PowderCell program and the FullProf program as described elsewhere.[3, 4] HR-TEM examinations of the $LiNi_{0.6}Co_{0.2}Mn_{0.2}O_2$ and Zr-doped materials was performed with a JEOL JEM-2100 (LaB_6) high resolution electron microscope, and convergent beam electron diffraction (CBED) technique (4 - 7 nm probe size) was employed for structural characterization of the obtained nano-particles. Samples for the TEM studies were prepared by methodology described in ref.[5]

2. Phase behavior on Li de-intercalation

The formation energies of the partially delithiated phase (Li_xMO_2) give direct indication of the phase behavior of cathode materials upon Li de-intercalation. The formation energies are calculated using the following equation:

$$E_F = E(Li_xMO_2) - xE(LiMO_2) - (1-x)E(MO_2) \quad \text{(S1)}$$

where $E(Li_xMO_2)$ is the total energy (per formula unit) of partially de-intercalated states, $E(LiMO_2)$ is the total energy of fully intercalated states and $E(MO_2)$ is the total energy of fully deintercalated states.

The results clearly show that Zr doping at Ni sites does not reduce the absolute formation energies (Figure S13). These results suggest that the phase stability of partially delithiated states are maintained on Zr doping and a solid solution of partially delthiated states is expected. Interestingly, the smooth experimental voltage profile confirms the above-suggested solid-solution behavior. On the other hand, Zr doping in the Li layer reduces the absolute formation energy, suggesting that significant amounts of Zr in the Li layer can reduce the phase stability of partially delithiated states. We also note that the magnitude of formation energies using the PBE+U method is lower than that obtained using the PBE method for NCM-622.

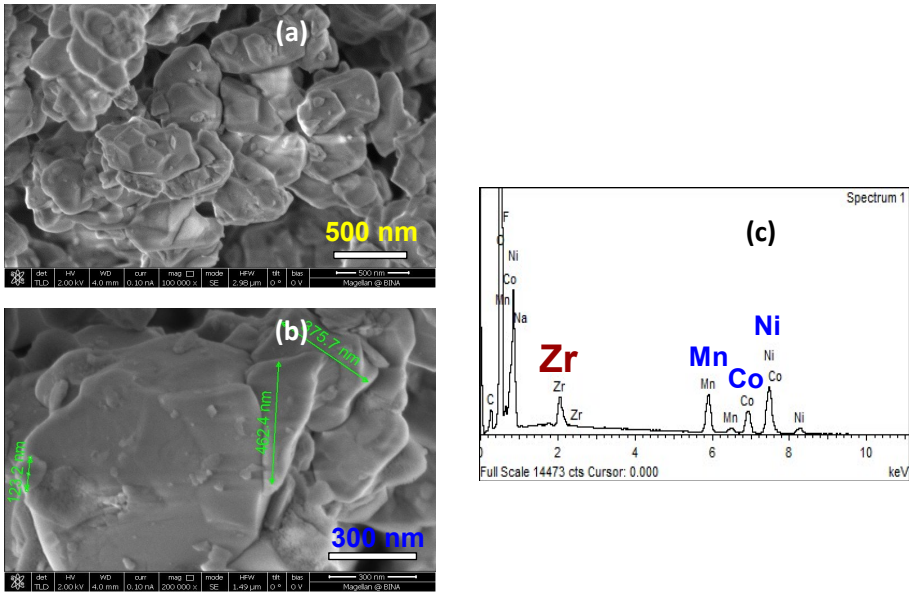

Figure S1. (a, b) Morphology of $LiNi_{0.6}Co_{0.2}Mn_{0.2}O_2$ doped with Zr (annealing at 900 °C, 1 h); (c) Energy-dispersive analysis spectrum of the Zr-doped NCM-622 material.

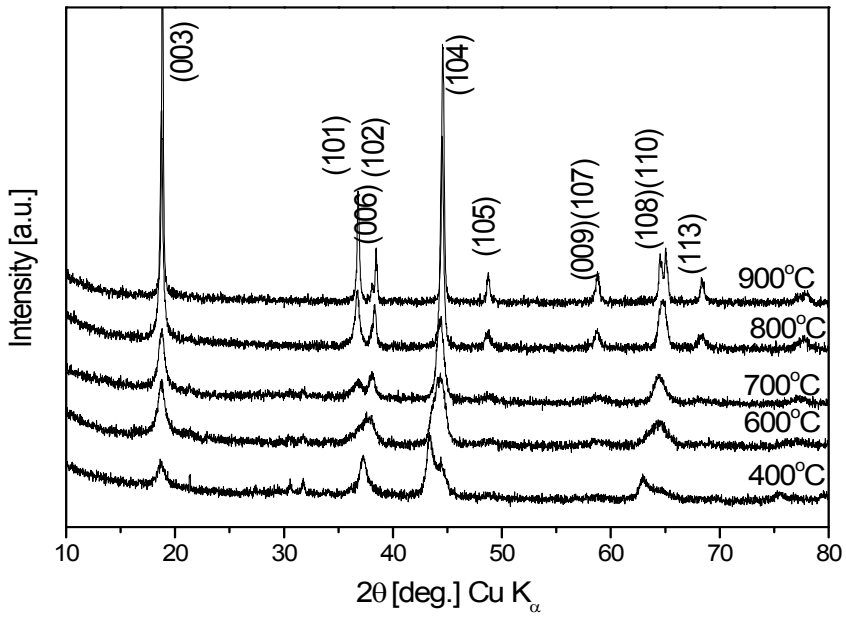

Figure S2. XRD patterns for $LiNi_{0.6}Co_{0.2}Mn_{0.2}O_2$ synthesized by the self-combustion reaction and subsequently thermally treated for 1 h at different temperatures (as indicated).

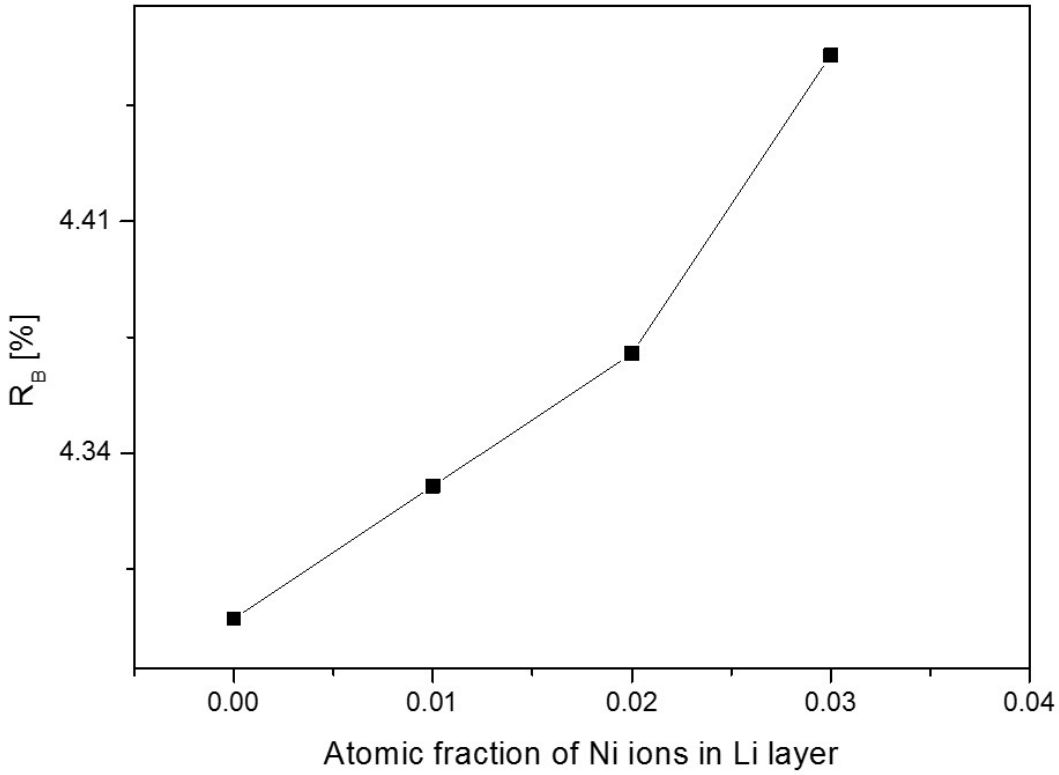

Figure S3. Variation of the R_{Bragg} factor with atomic fraction of Ni ions in the Li layer of $LiNi_{0.56}Zr_{0.04}Co_{0.2}Mn_{0.2}O_2$.

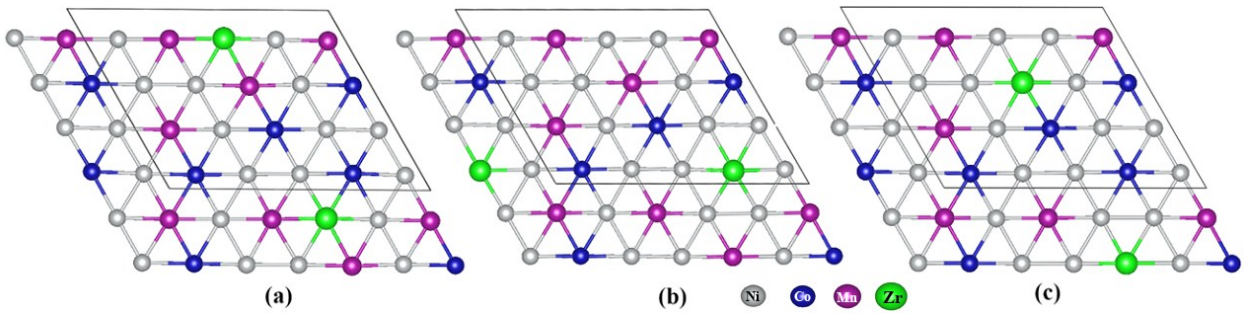

Figure S4. Most preferred substitution sites of Zr in $LiNi_{0.6}Co_{0.2}Mn_{0.2}O_2$: (a) Zr doping at Ni sites, (b) Zr doping at Co sites, (c) Zr doping at Mn sites. Only single metal layers are shown for the sake of simplicity, although the calculations were performed using large supercells (240 atoms, 60 formula units).

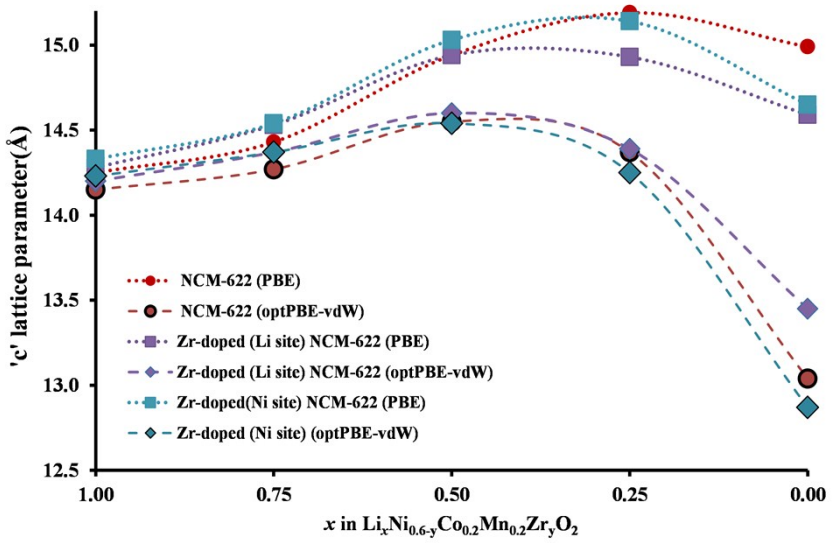

Figure S5. The change in *c* lattice parameter for pristine and Zr-doped NCM-622 with Li concentration using PBE and dispersion-corrected PBE. y=0.05 for Zr doped (at Ni-sites in both TM and Li layers) and y=0.00 for pristine NCM-622.

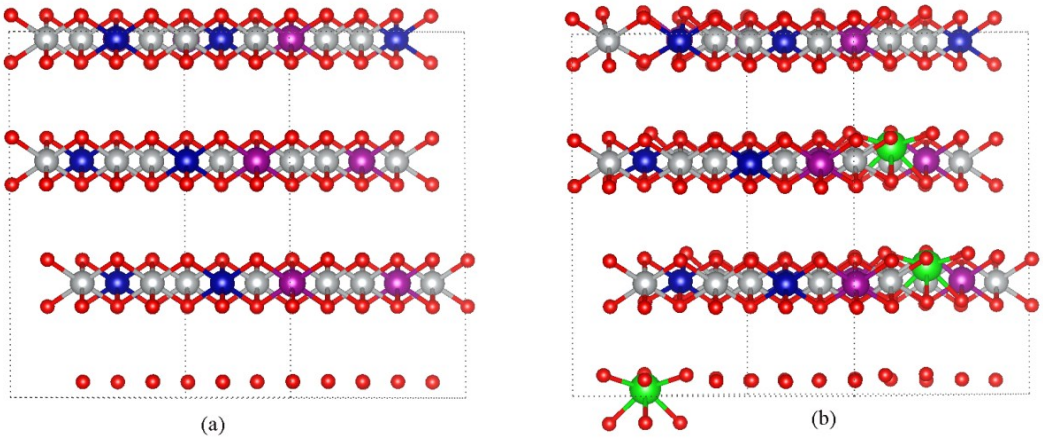

Figure S6. The relaxed structure of fully delithiated supercells (a) $Ni_{0.6}Co_{0.2}Mn_{0.2}O_2$ and (b) $Ni_{0.55}Co_{0.2}Mn_{0.2}Zr_{0.05}O_2$ using the PBE method. Color codes for spheres: red-oxygen atoms and grey-Ni atoms, violet-Mn atoms, blue-Co atoms.

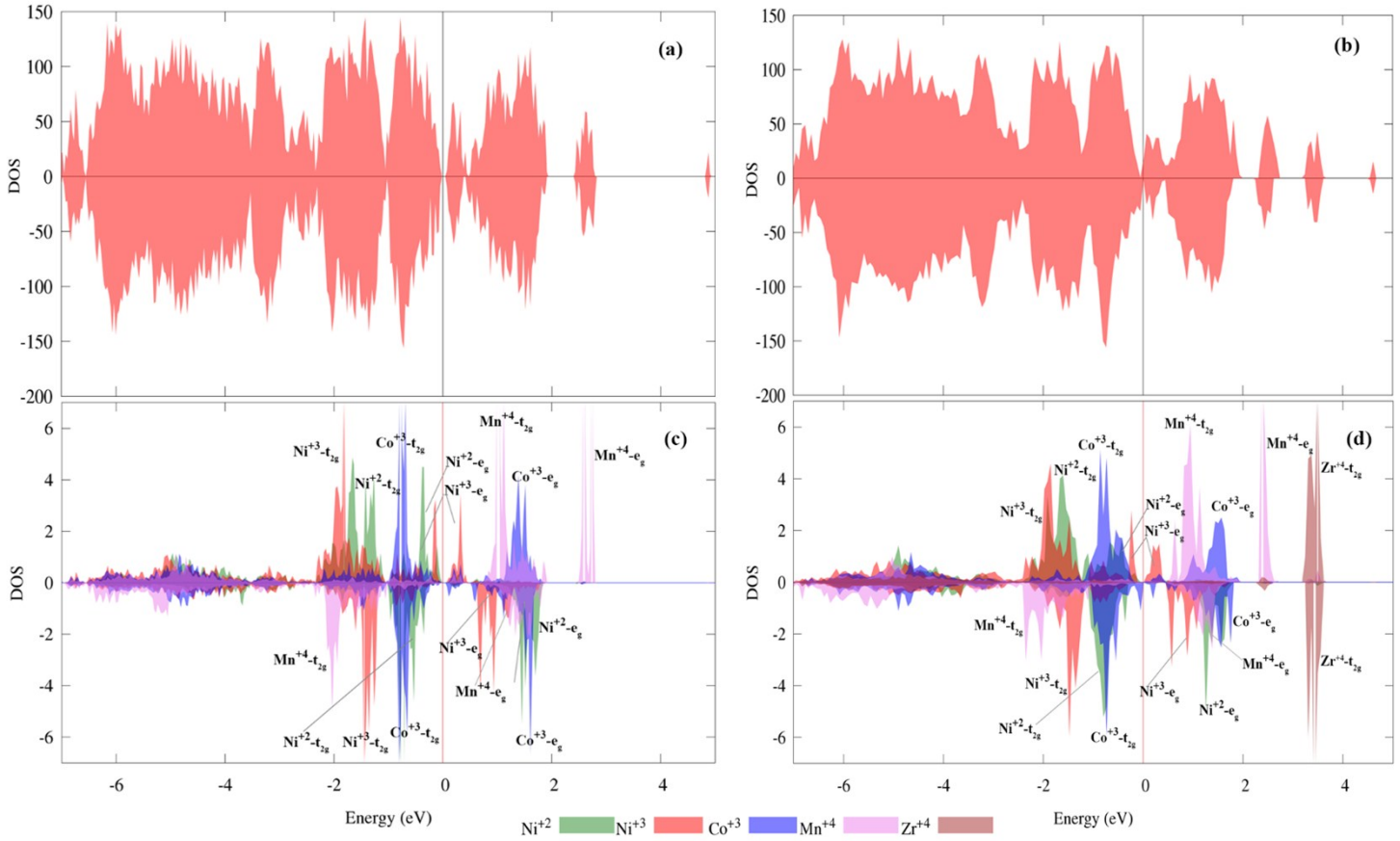

Figure S7. (a) Total DOS for $LiNi_{0.6}Co_{0.2}Mn_{0.2}O_2$ (b) Total DOS for $LiNi_{0.55}Co_{0.2}Mn_{0.2}Zr_{0.05}O_2$ (c) PDOS for $LiNi_{0.6}Co_{0.2}Mn_{0.2}O_2$ (d) PDOS for $LiNi_{0.55}Co_{0.2}Mn_{0.2}Zr_{0.05}O_2$ using the PBE method.

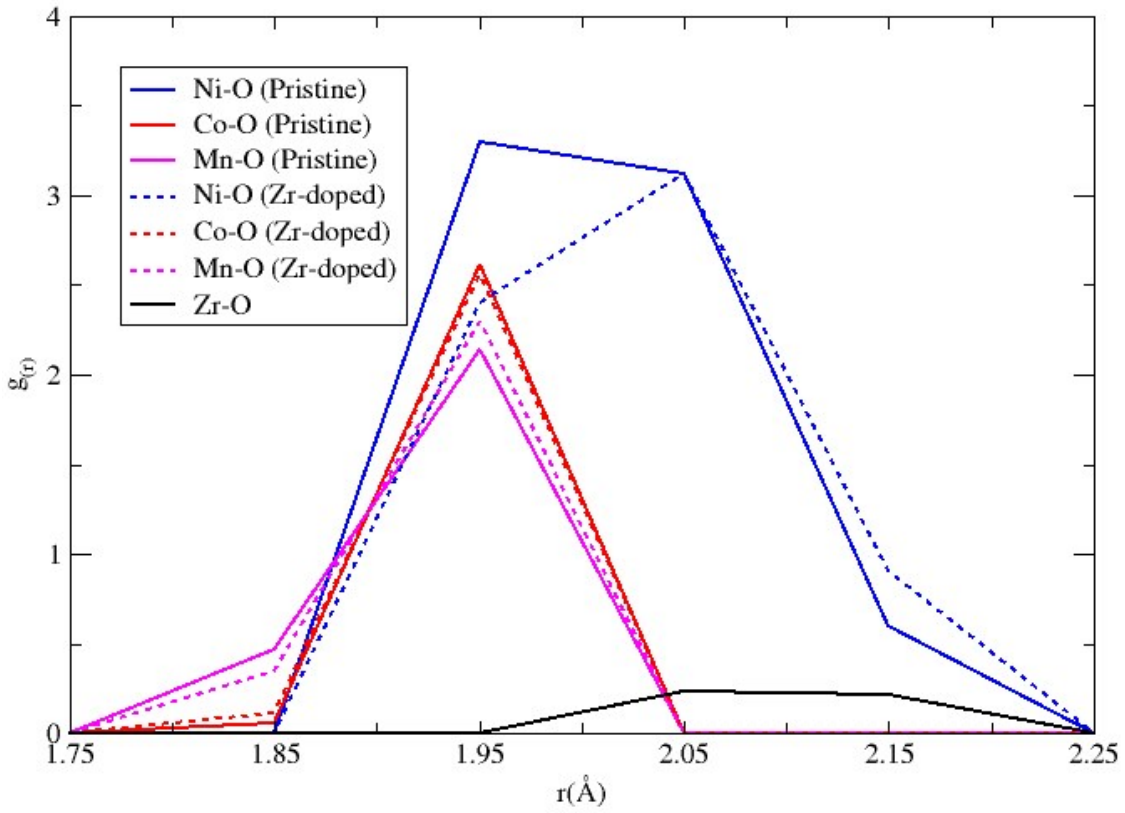

Figure S8. Radial pair distribution function (TM-O) of the relaxed structure of pristine and Zr-doped NCM-622 using the PBE method.

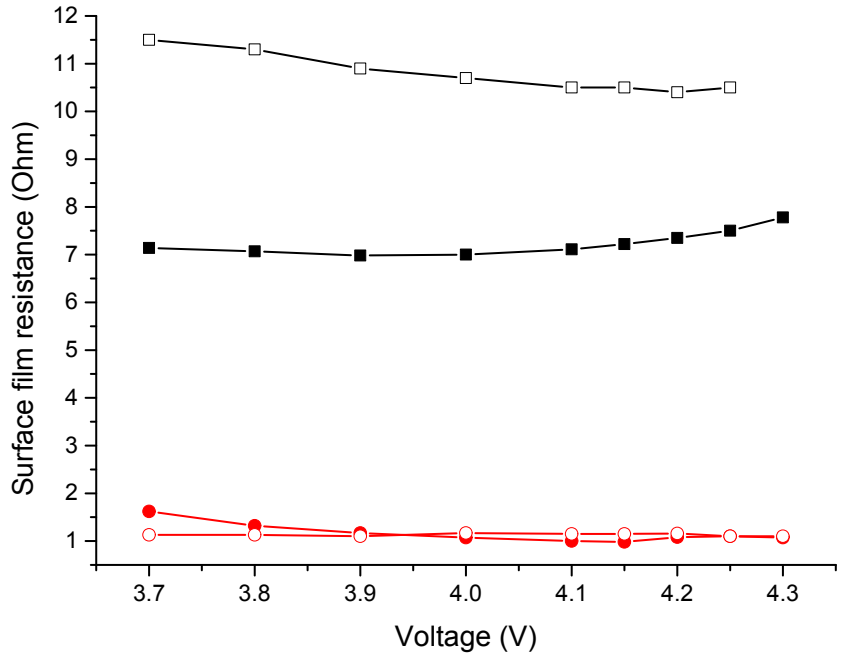

Figure S9. Surface film resistance measured from impedance spectra of electrodes comprising undoped NCM-622 and Zr doped NCM-622 (black and red curves, respectively) after 5 CVs and after 50 consecutive galvanostatic cycles at a C/5 rate, 45^0C (filled and empty symbols, respectively).

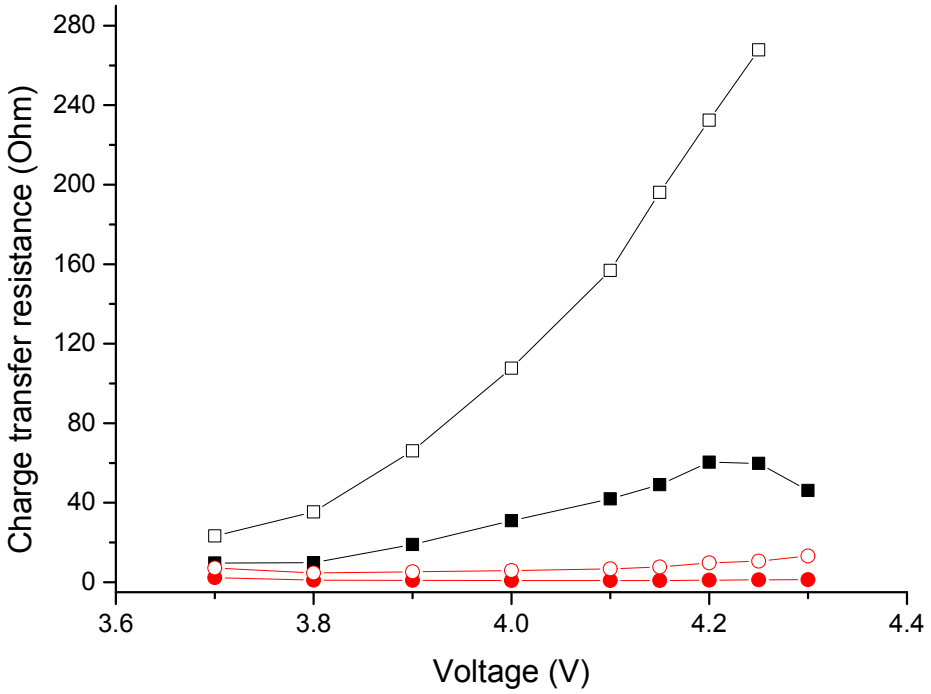

Figure S10. Charge transfer resistance measured from impedance spectra of electrodes comprising undoped NCM-622 and Zr doped NCM-622 (black and red curves, respectively) after 5 CVs and after 50 consecutive galvanostatic cycles at a C/5 rate, 45^0C (filled and empty symbols, respectively).

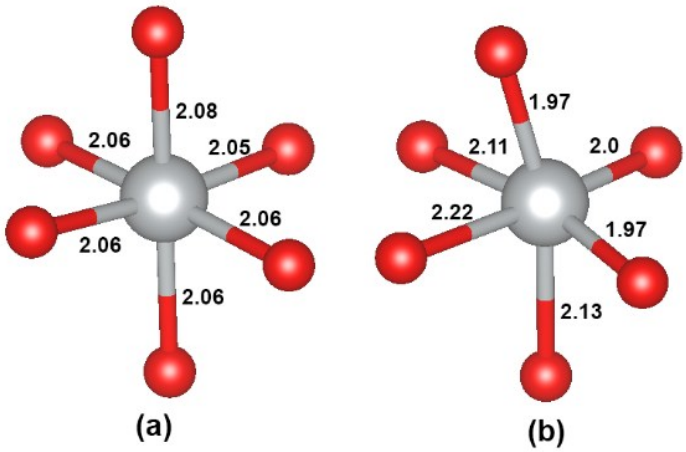

Figure S11. Structure of NiO_6 octahedra of migrating Ni^{2+} in (a) fully lithiated NCM-622 (b) NCM-622 with 4 Li vacancies (3 vacancies near migrating Ni and one vacancy at final migrating site). Color codes for spheres: red-O atoms and grey-Ni atoms.

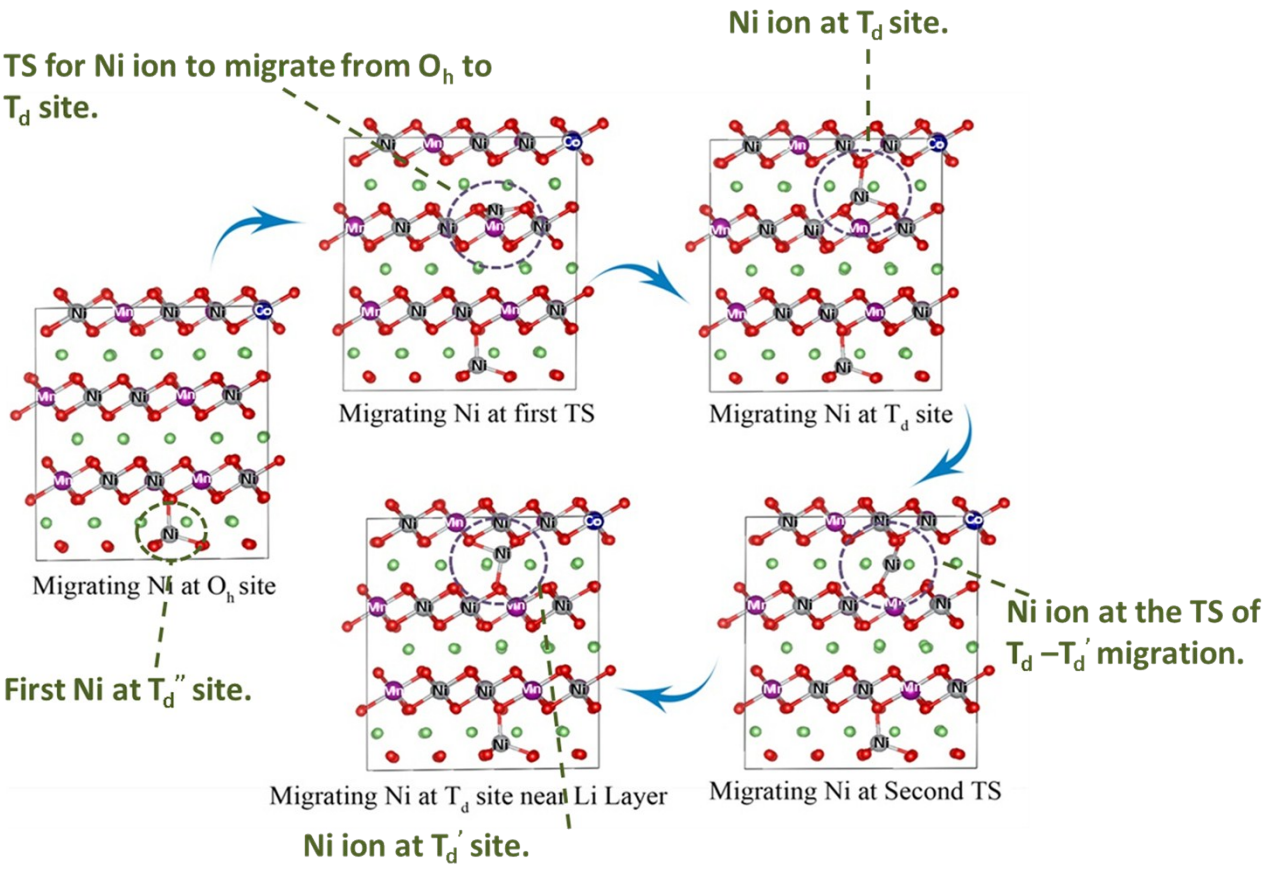

Figure S12. Schematic Ni^{2+} migration path in undoped NCM-622. Color codes for spheres: red-oxygen atoms, grey-Ni atoms, violet-Mn atoms, blue-Co atoms and green-Li atoms.

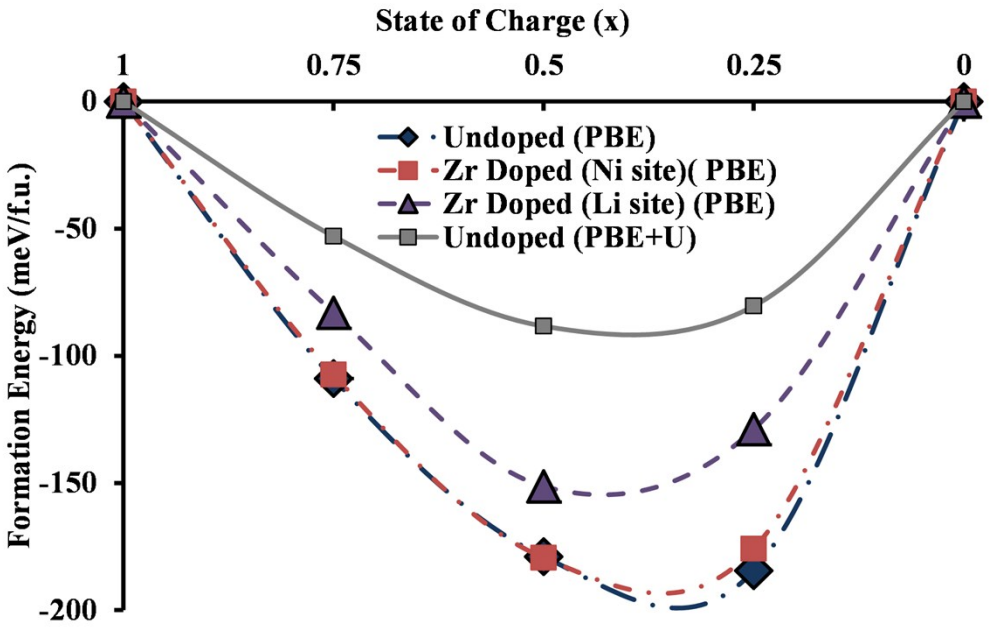

Figure S13. Calculated formation energies of undoped and Zr-doped NCM-622 at different lithium de-intercalation levels.

Table S1. The *a* and *c* lattice-parameters for undoped $LiNi_{0.6}Co_{0.2}Mn_{0.2}O_2$, Zr-doped $LiNi_{0.56}Zr_{0\cdot04}Co_{0.2}Mn_{0.2}O_2$ pristine materials and those of electrochemically cycled electrodes, as obtained from the XRD data.

	Undoped (Å)	Zr-Doped (Å)
Pristine materials	*a*=2.8703, *c*=14.2134	*a*=2.8709, *c*=14.2264
After 50 cycles, terminated at 4.3 V (charged state)	*a*=2.8278, *c*=14.3431	*a*=2.8218, *c*=14.3365

References

1. D. Kovacheva, H. Gadjov, K. Petrov, S. Mandal, M. G. Lazarraga, L. Pascual, J. M. Amarilla, R. M. Rojas, P. Herrero and J. M. Rojo, *Journal of Materials Chemistry*, 2002, **12**, 1184-1188.
2. S. K. Martha, E. Markevich, V. Burgel, G. Salitra, E. Zinigrad, B. Markovsky, H. Sclar, Z. Pramovich, O. Heik, D. Aurbach, I. Exnar, H. Buqa, T. Drezen, G. Semrau, M. Schmidt, D. Kovacheva and N. Saliyski, *Journal of Power Sources*, 2009, **189**, 288-296.
3. W. Kraus and G. Nolze, *Journal of Applied Crystallography*, 1996, **29**, 301-303.
4. J. Rodríguez-Carvajal, *Physica B: Condensed Matter*, 1993, **192**, 55-69.
5. H. Gabrisch, T. Yi and R. Yazami, *Electrochemical and Solid-State Letters*, 2008, **11**, A119-A124.